International Journal of Civil and Structural Engineering– IJCSE
Volume 2 : Issue 2 *[ISSN : 2372-3971]*
Publication Date: 19 October, 2015

Resistance of rectangular concrete-filled tubular sections to the combined axial compression and bending

[Young Bong Kwon, Sung Woong Park and In Kyu Jeong]

***Abstract*—This paper describes the development of the direct strength method (DSM) for concrete-filled tubular (CFT) sections. A formula for strength interactions of CFT members under combined compression and flexure is proposed and is compared with test results. The comparison confirmed that the formula for axial and flexural strength and that for strength interactions can conservatively predict the resistance of CFT columns to the axial load and combined compression and bending.**

***Keywords*—Rectangular Concrete-Filled Tubular (CFT) Sections, Resistance, Combined Compression and Axial Bending, Direct Strength Method (DSM)**

I. Introduction

Since concrete-filled tubular (CFT) sections have advantages such as high strength, excellent ductility, and large energy dissipation capacity, they are used as structural members for high-rise buildings and long-span bridges. Since the steel skin confines the outward deformation of the filled-in concrete and the concrete resists the inward deformation of the steel skin, both steel and concrete enhance the strength of CFT sections. However, the thin steel skin of CFT sections is susceptible to elastic or inelastic local buckling under compression and/or bending before overall buckling or material yielding. However, there is substantial post-buckling strength in the local buckling mode, and this should be accounted for in estimating the design strength of the steel skin. An increase in the compressive strength of concrete from tri-axial confinement by the locally buckled steel skin should also be considered in estimating the ultimate strength of CFT sections.

The present paper proposes a set of squash load equations for circular and rectangular CFT columns to account for the local buckling of the steel skin based on previous compression test results for CFT sections in the literatures. The predicted squash load of CFT columns is compared with test results and those predicted by existing specifications. In addition, the paper also proposes a simple formula for flexural strength for the direct strength method (DSM) based on the sectional slenderness of the steel skin of CFT sections.. All strength curves use the elastic local buckling stress of the steel skin, which can be computed by a rigorous analysis program or theoretical equations, and a limiting strength formula based on various test results. The paper proposes and compares strength interaction equations with test results under eccentric loading. The comparison confirmed that the proposed formula for axial and flexural strength and interaction equations can conservatively predict the strength of CFT columns. .

Young Bong Kwon and Sung Woong Park
Yeungnam University
Korea (Rep.)

In Kyu Jeong
Korea Rural Community Corporation
Korea (Rep.)

II. Resistance of CFT columns to axial compression

A squash load equation for circular and rectangular CFT section stub columns for the DSM has been proposed based on various test results in Kwon et al. [1]. The equation proposed adopted a single formula for both circular and rectangular CFT section columns. However, since the axial resistance of rectangular sections based on the elastic local buckling stress is very different from that of circular sections and thus produces too conservative estimates for rectangular CFT sections, it needs to be expressed in a different formula for the better estimation of axial strength.

A formula for the axial resistance of rectangular CFT stub columns can be given by

$$P_{no} = \varphi_s F_{sd} \cdot A_s + \varphi_c C_2 \cdot f_c \cdot A_c \quad (1)$$

where F_{sd} = steel design stress; A_s =steel area; f_c =concrete compressive strength; A_c = concrete area; A_{sr} =steel reinforcement bar area; F_{yr} = yield stress of steel bar; and φ_s and φ_c are material factors for steel and concrete and taken as 0.95 and 0.65, respectively. The format of the resistance formula is quite similar to that in EC4 [3]. The portion of the reinforcement steel bar for axial resistance is omitted in Eq. (1) for simplicity.

The design strength formula for welded steel sections [2] can be conservatively adopted for the steel skin of rectangular CFT columns. The design strength curves for a rectangular steel skin to account for local buckling are given by

$$F_{sd} = F_y \quad \text{for } \lambda \le 0.816 \quad (2a)$$

$$F_{sd} = [1 - 0.15(\frac{F_{crl}}{F_y})^{0.5}](\frac{F_{crl}}{F_y})^{0.5} F_y$$

For $0.816 < \lambda \le 2.5$ (2b)

where

$$\lambda = \sqrt{\frac{F_y}{F_{crl}}} \quad (2c)$$

The elastic local buckling stress F_{crl} can be computed by rigorous computer programs or a theoretical local buckling stress equation. The theoretical elastic local buckling stress formula for a simply supported plate given in Eq. (3) can be used for square sections and rectangular sections composed of equal-width subpanels [3]:

$$F_{crl} = \frac{4\pi^2 E}{12(1-\nu^2)}\left(\frac{t}{b}\right)^2 \quad (3)$$

where t= thickness and b= width of the plate or subpanel. Since the width and height of a rectangular section are not equal, Eq. (3) cannot be directly used. The equivalent width in Eq. (4) can be adopted to calculate an elastic local buckling stress using Eq. (3).

$$\frac{b_{eq}}{t} = \frac{1}{4}\frac{b_1}{t} + \frac{3}{4}\frac{b_2}{t} \quad (4)$$

III. Flexural strength of CFT sections

The stress distribution of rectangular CFT sections in flexure for compact, noncompact, and slender (called slender after here because there is no limit between noncompact and slender section in DSM) is quite similar to fully plastic theory and is given in Fig. 1. The compressive stress of the steel skin should be determined according to Eqs. (2a) and (2b) using the elastic local buckling stress under pure bending. As shown in Fig. 1, for compact sections($\lambda \le 0.816$), the compressive stress in Eq. (2a) of the steel skin reaches the yield stress of the material, and the tensile stress also reaches it. The concrete stress is assumed as cube strength with the material factor applied. For slender sections ($0.816 < \lambda \le 2.5$), the compressive stress of the steel skin does not reach the nominal yield stress of the material according to Eq. (2b), whereas the tensile stress reaches it. However, because the steel section in compression is assumed to sustain its post-buckling strength until its final failure, the stress block can be assumed as similar to the stress block for a compact section. The concrete strength factor can be computed by Eqs. (5a) and (5b).

$$C_2 = 1.0 \quad \text{for } \lambda \le 0.816 \quad (5a)$$

$$C_2 = 1.0 - 0.65(\lambda - 0.816)^2 \quad \text{for } 0.816 < \lambda \quad (5b)$$

In the calculation of C_2 and F_{sd} for the flexural resistance of CFT sections, the elastic local buckling stress F_{crl} should be determined under pure bending instead of under uniform compression, which can be computed by the FEM or FSM program. However, Eq. (3) can be used conservatively for the simple calculation of design compressive strength and concrete strength factor .

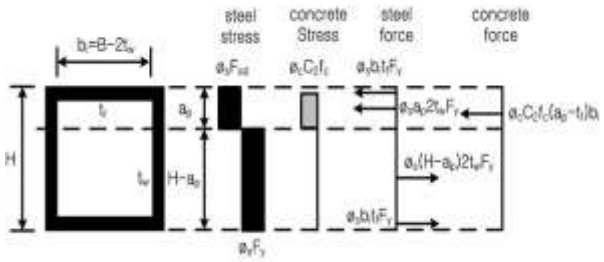

Fig. 1. Stress distribution of rectangular CFT sections

IV. Resistance to combined compression and uniaxial bending

A. *Strength interaction formula*

In general, an accurate strength interaction curve obtained by the strain compatibility method should be used to check the resistance of CFT columns under combined axial force and bending. However, because this method requires stress-strain relationships for concrete and steel and repetitive calculations, it is inconvenient, and therefore a simplified interaction curve has been adopted to determine the resistance of columns to combined compression and bending under EC4 [4] and AISC specifications [5]. Fig. 8 shows the simplified strength interaction curves, which are quite similar to those in EC4 and AISC specifications, except for the replacement of F_{sd} for F_y in the compression zone. For compact sections, strength interaction curves defined in the DSM, EC4, and AISC specifications are quite simple because they are based on the theory of the fully plastic moment. In addition, strength interaction equations can be defined in a similar manner for slender sections. Fig. 2 shows strength interaction curves for compact and slender sections. The design compressive stress F_{sd} at point A is computed using the elastic local buckling stress based on the uniform compressive load and at B based on pure bending, as mentioned earlier. Therefore, the compressive stress F_{sd} at points C and D can be linearly interpolated between those values at points A and B according to the axial force. The stress F_{sd} at point C can be obtained by

$$F_{sd} = F_{sd,A} + (F_{sd.B} - F_{sd,A})\frac{(P_A - P_C)}{P_A} \quad (6)$$

where $F_{sd,A}$ and $F_{sd,B}$ are steel design stresses at points A and B, respectively.

Similarly, the concrete strength factor C_2 at point A is computed using the elastic local buckling stress under uniform compression, and that at point B is obtained under pure bending. Those values at points C and D can be computed similarly through a linear interpolation between those values at points A and B according to the ratio of the compression force. However, if interpolated values are used for F_{sd} and C_2, then the safety check procedure becomes much more difficult. For the simplified strength computation, F_{sd} and C_2 at points C and D are assumed as values at point B.

The flexural moment M_B at point B is a pure bending moment, and the moment M_C at point C is the same as M_B at point B. Therefore, the axial force P_C can be computed by the sum of the resulting force at point B and that at point C. The axial force P_C is the combined steel and concrete force given by

$$P_C = \varphi_c C_2 f_c A_c - (\varphi_s F_y - \varphi_s F_{sd}) A_s \quad (7)$$

Because F_{sd} is equal to F_y for compact sections, the axial force is the plastic resistance of concrete alone, and Eq. (7) can be expressed as

$$P_C = \varphi_c C_2 f_c A_c \quad (8)$$

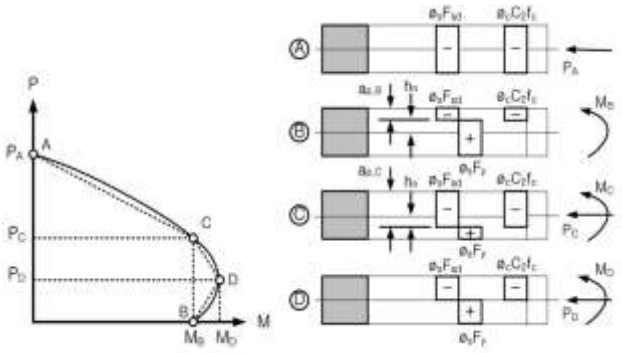

Fig. 2.Compression-uniaxial bending strength interaction curve

Because the neutral axis is located on the centroid of the CFT section at point D, the axial force P_D is a half of P_C, as shown in Fig. 2:

$$P_D = \frac{P_C}{2} = \frac{1}{2}[\varphi_c C_2 f_c A_c + (\varphi_s F_y - \varphi_s F_{sd}) A_s] \quad (9)$$

The distance from the centroid to the neutral axis can be obtained by comparing the stress distribution at points B and C:

$$h_n = \frac{P_C}{2 b_i \varphi_c f_c + 4t(\varphi_s F_y + \varphi_s F_{sd})} \quad (10)$$

Once h_n is calculated, the moments at points B, C and D can be calculated easily.

Flexural strength at point D is the maximum moment and can be calculated by

$$M_D = \frac{Z_{ps}}{2}(\varphi_s F_{sd} + \varphi_s F_y) + \frac{Z_{ps}}{2}\varphi_c f_c \quad (11a)$$

where

$$Z_{pc} = \frac{(b_i)(H-2t)^2}{4} \quad (11b)$$

$$Z_{ps} = \frac{BH^2}{4} - Z_{pc} \quad (11c)$$

The flexural strength at point B, which is pure bending, can be calculated by

$$M_B = M_D - \frac{Z_{pcn}}{2}\varphi_c f_c - \frac{Z_{psn}}{2}(\varphi_s F_{sd} + \varphi_s F_y) \quad (12a)$$

where

$$Z_{pcn} = b_i h_n^2 \quad (12b)$$

$$Z_{psn} = 2t h_n^2 \quad (12c)$$

Although an additional point can be added between points A and C for a more accurate estimation of resistance, a simplified strength interaction curve can generally be completed by connecting points A, C, B, and D directly and the linear interpolation between them. In reality, however, the moment resistance at point D is slightly higher than that at point C for slender sections. Therefore, the resistance at point D can be neglected, and an interaction curve can be obtained by removing D and connecting point B to point C directly in the interaction curve, as shown in Fig. 2.

B. *Comparison with test results*

The strength equation in previous sections should be modified to account for column slenderness relative to test results. Moment strength is left as it is, whereas axial strength in the strength interaction curve is reduced by using the slenderness reduction factor in AISC specifications [4] to account for column slenderness. The axial force at points A, C, and D in Figs. 3 and 4 indicates the reduced strength of the squash load of stub columns by multiplication with the slenderness reduction factor, which is a ratio of column strength to the squash load:

$$\alpha = \frac{P_n}{P_{no}} \tag{13}$$

where P_n is column strength computed by Eqs. I2-2 and I2-3 in AISC specifications [4].

The reduced strength interaction curve is compared with the test results in [6-7] in Figs. 3 and 4 for verification purposes. In addition, strength interaction curves in AISC specifications and EC4 are included in Figs. 3 and 4 for comparison purposes. As shown in Figs. 3 and 4, the reduced strength interaction curve shows conservative resistance for test columns in combined axial compression and bending in comparison with test results for CFT section columns in [6, 7]. The strength prediction of columns under combined compression and bending is more conservative than that under the axial load or pure bending alone. Because the test columns in [6] are stub columns, the reduction in strength due to column slenderness is negligible. The AISC strength interaction curve is much more conservative than the DSM curve for all sections of 20 in b/t and similar for the sections of 30 in b/t. However, the AISC strength interaction curve is slightly less conservative than the DSM curve for the sections of 40 in b/t. The test yield stress, ultimate stress, and compressive concrete strength of test specimens in [6] are 750.0 MPa, 817 MPa, and 28~32 MPa, respectively, and the width-to-thickness ratios are 20, 30, and 40. In AISC specifications, sections with a width-to-thickness ratio of 30 and 40 are classified as non-compact sections, that is, whose slenderness exceeds 0.816. As shown in Fig. 4, the strength interaction curve conservatively predicts the strength of CFT columns under compression and bending in comparison with test results in [7]. The EC4, AISC and DSM strength interaction curves are quite similar for all sections with a width-to-thickness ratio of 35.3 that are compact sections. However, for the sections with a width-to-thickness ratio of 52.2, DSM strength interaction curves are much less conservative, because AISC specifications adopts the interaction curve for steel members. Sections whose width-to-thickness ratios equal to 52.2 are noncompact sections in AISC specifications, whereas the others are compact sections. The yield stresses of Varma's test [7] are 269 MPa, 471 MPa, whereas the concrete strength is 110 MPa in all cases. Regardless of width-to-thickness ratio, all test sections failed, mainly because of the bending moment.

As shown in Figs. 3 and 4, the proposed strength interaction curve shows conservative strength estimates under the axial load, the bending moment, and combined axial compression and uniaxial bending in comparison to various test results. Regardless of the width-to-thickness ratio of the steel skin, the strength estimates and interaction equations for CFT columns are verified to be reasonably conservative. Although the steel design stress F_{sd} and the concrete strength factor C_2 computed based on the local buckling stress of the steel skin under the pure bending condition is employed for the case of combined axial compression and bending, the resistance according to the reduced strength interaction curve shows reasonably conservative values. The results in Figs. 3 and 4 verify that the stress assumptions for axial compression, pure bending, and combined axial compression and bending for both compact and slender sections are quite reasonable for design purposes.

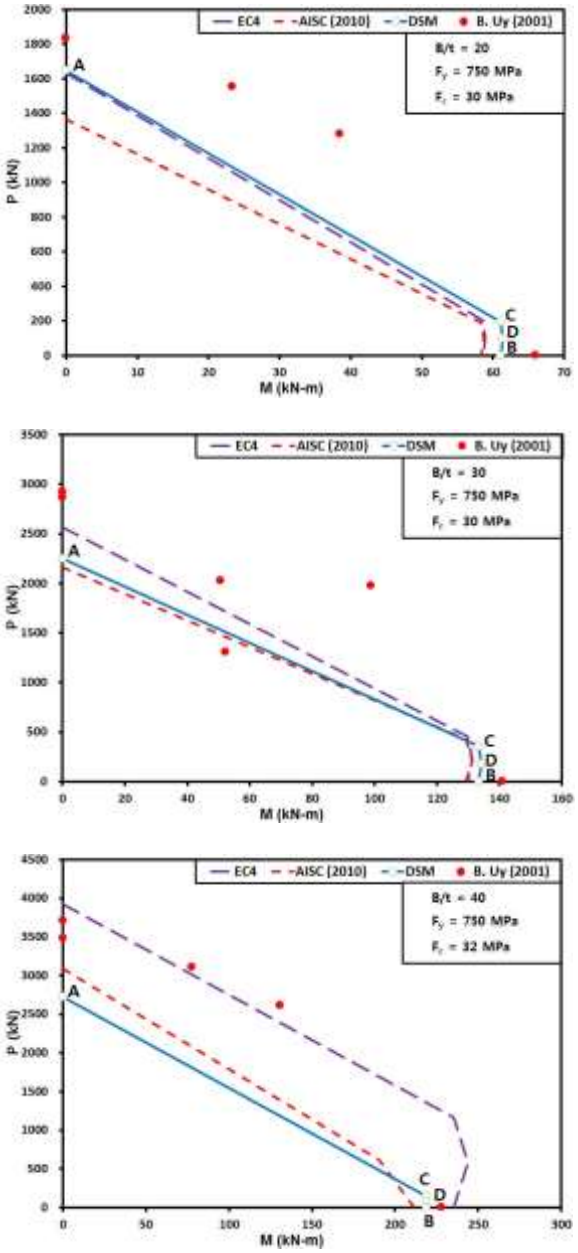

Fig. 3. Compression of strength interaction curve and test results [6]

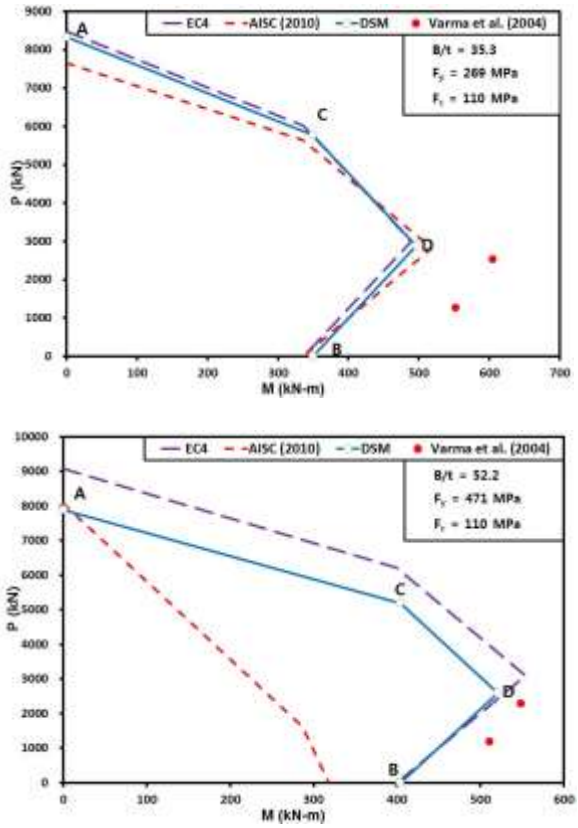

Fig. 4. Compression of strength interaction curve and test results [4]

Acknowledgment

This paper forms a part of the project entitled "Development of a Direct Strength Method for Welded Sections" being conducted in the Department of Civil Engineering at Yeungnam University. This research was supported by the 2013 research fund (no. 2012R1A1B3002777) of the National Research Foundation of Korea.

References

[1] Kwon YB, Gang DW, Seo SJ. Prediction of the ultimate strengths of concrete-filled tubular section columns, Thin-Walled Structures 2011; 49: 85-93.

[2] Kwon YB. The development of Direct Strength Method for welded steel members with local buckling, Thin-Walled Structures 2014; 81: 121-131.

[3] European Committee for Standardisation (ECS), Eurocode 4: Design of Composite Steel and Concrete Structures, Part 1-1: General rules and rules for buildings, Brussels, Belgium, 2004.

[4] American Institute of Steel Construction (AISC), Specification for Steel Structural Buildings, Chicago, Il, USA, 2010.

[5] Timoshenko SP.,Gere JN. Theory of elastic stability, New York; McGraw-Hill, 1961.

[6] Uy B. Strength of short concrete filled high strength steel box columns, Journal of Constructional Steel Research, Volume 57, Issue 2, 2001, pp.113-134.

[7] Varma AH, Ricles JM, Sauce R. Lu LW. Seismic behavior and design of high-strength square concrete-filled steel tube beam columns, Journal of Structural Engineering, ASCE, Vol. 1130, No.2, 2004, pp.169-179.

About Author (s):

Simplified method for the strength interaction curve of axial compression and bending of concrete-filled tubular (CFT) sections is proposed. Axial and flexural strength formulae are proposed for the Direct Strength Method.